



Published in final edited form as:

*J Neurosci Methods*. 2018 June 01; 303: 169–177. doi:10.1016/j.jneumeth.2018.03.019.

## EEG-based neglect assessment: A feasibility study

Aya Khalaf<sup>a,\*</sup>, Jessica Kersey<sup>b,1</sup>, Safaa Eldeeb<sup>a,1</sup>, Gazihan Alankus<sup>c</sup>, Emily Grattan<sup>d</sup>, Laura Waterstram<sup>b</sup>, Elizabeth Skidmore<sup>b</sup>, Murat Akcakaya<sup>a</sup>

<sup>a</sup>Electrical and Computer Engineering, University of Pittsburgh, 3700 O'Hara St, Pittsburgh, PA 15213, USA

<sup>b</sup>Department of Occupational Therapy, University of Pittsburgh, 5012 Forbes Tower, Pittsburgh, PA 15260, USA

<sup>c</sup>Department of Computer Engineering, Izmir University of Economics, Sakarya Cd. 156, 35330, Turkey

<sup>d</sup>Department of Health Sciences and Research, Medical University of South Carolina, 77 President Street, MSC 700, Charleston, SC 29425, USA

### Abstract

**Background:** Spatial neglect (SN) is a neuropsychological syndrome that impairs automatic attention orienting to stimuli in the contralesional visual space of stroke patients. SN is commonly assessed using paper and pencil tests. Recently, computerized tests have been proposed to provide a dynamic assessment of SN. However, both paper- and computer-based methods have limitations.

**New method:** Electroencephalography (EEG) shows promise for overcoming the limitations of current assessment methods. The aim of this work is to introduce an objective passive BCI system that records EEG signals in response to visual stimuli appearing in random locations on a screen with a dynamically changing background. Our preliminary experimental studies focused on validating the system using healthy participants with intact brains rather than employing it initially in more complex environments with patients having cortical lesions. Therefore, we designed a version of the test in which we simulated SN by hiding target stimuli appearing on the left side of the screen so that the subject's attention is shifted to the right side.

**Results:** Results showed that there are statistically significant differences between EEG responses due to right and left side stimuli reflecting different processing and attention levels towards both sides of the screen. The system achieved average accuracy, sensitivity and specificity of 74.24%, 75.17% and 71.36% respectively.

**Comparison with existing methods:** The proposed test can examine both presence and severity of SN, unlike traditional paper and pencil tests and computer-based methods.

**Conclusions:** The proposed test is a promising objective SN evaluation method.

\*Corresponding author. afk17@pitt.edu (A. Khalaf).

<sup>1</sup>Both authors contributed equally to this manuscript.

## Keywords

Stroke; Spatial neglect; Attention; Electroencephalography; Classification; Computer-aided diagnosis

---

## 1. Introduction

Every year, 15 million people around the world experience stroke including 795,000 cases in the United States (CDC and NCHS, 2015). The consequences of a stroke are strongly related to the lesion volume and its location in the brain (Agis et al., 2016). Such consequences may range from minor problems such as headache up to significant complications in which individuals may experience cognitive, motor, visual, or affective impairments. Examples on these impairments include: sudden weakness, vision problems, difficulty in speaking, loss of memory, or paralysis on the side of the body opposite to the affected brain hemisphere (Donnan et al., 2008).

Spatial neglect (SN) is a neuropsychological syndrome that is one of the most common consequences of right-side brain damage after stroke (Heilman et al., 1993), occurring in 28.60% of the stroke population (Becker and Karnath, 2007). SN occurs as a result of brain lesions in the right inferior parietal cortex, the superior temporal cortex or the ventral frontal cortex (Committeri et al., 2007). In addition, it can occur due to disconnections in attentional networks (Baldassarre et al., 2014). Patients with SN are characterized by their inattention to stimuli that appear on their contralesional side which was thought usually to be the left visual side (Li and Malhotra, 2015). However, it was shown later that right-sided SN can be found with higher percentage using multitasking (Blini et al., 2016a). An individual with left-sided SN may demonstrate difficulties such as inability to focus attention on the left, missing food found on the left side of the plate, missing words on the left side of the page while reading, forgetting to dress the left side of the body, getting confused by moving objects and fear of walking in crowded places (Unsworth, 2006).

During the last few decades, many paper and pencil tests have been used to assess SN (Plummer et al., 2003). The Behavioral Inattention Test (BIT) is one of the most commonly used SN assessment methods and includes tasks such as line crossing, line bisection, letter and star cancellation, copying and drawing symmetric figures (Wilson et al., 1987). One drawback of such tests is that they are static. In other words, the objects shown on the page are stationary so they do not reflect the dynamic nature of objects in the real life (Seki and Ishiai, 1996). In addition, the evaluation of some tests like copying and drawing figures leaves room for error and variations in interpretation and scoring among raters. Furthermore, the variability in performance on paper and pencil tasks is relatively high. For example, an individual with SN may perform normally on a line bisection test but demonstrate impairment on star cancellation or vice versa. As a result of these combined limitations, an individual with SN may not meet criteria for SN on these tests, but nonetheless SN is observed while they are engaged in functional activities such as eating, dressing, or walking through a crowded place. Recently, computerized tests for SN assessment have been proposed and developed to address these shortcomings (Pedroli et al., 2015). Such tests have

the potential to highlight SN cases which often go undetected by paper-and-pencil tests (Bonato and Deouell, 2013).

Passive BCI is mainly concerned with monitoring and interpreting user's brain activity (Zander and Kothe, 2011) unlike active BCI, it is not designed for voluntary control. Passive BCI concept is employed in many applications such as measuring working memory load (Grimes et al., 2008), assessing driver's vigilance state (Schmidt et al., 2009), and assessing attention (Brouwer et al., 2013). In this paper, we introduce a novel electroencephalography (EEG)-based passive BCI system that can be used as a robust and objective SN assessment test. This test may provide additional benefits beyond what current assessment methods provide. First, the EEG system has the potential to provide a visual map of the areas being attended to by the patient by identifying targets that were not attended to within the available field of vision. This provides more precise information about the severity of peripersonal and extrapersonal visual neglect. Many current assessment methods provide only sufficient information to diagnose SN, and limited detail on its severity. Therefore, EEG assessment can address a component of assessment that is missing from current approaches. Additionally, the EEG assessment system has the potential to automate SN assessment, updating in real-time on an ongoing basis, with easier repeatability than paper and pencil tests. With further development, this test can be integrated into functional daily tasks to provide an assessment of SN within a dynamic and natural setting. Particularly, we will integrate this EEG test into a virtual-reality based intervention in which real-time EEG readings will trigger visual and tactile cues when visual cues are missed on the neglected side. Finally, EEG has the potential to examine the presence and severity of SN in both acute and chronic stroke, as there is no learning effect or timing effect. In this test, EEG signal is recorded while the participants observe visual stimuli illustrated on a screen at random locations. These visual stimuli include both targets and distractors that change overtime independently of each other. We performed a feasibility study to show the performance of the system through the participation of healthy individuals. The aim behind starting the experiments with healthy participants is to validate the proposed system under less complex conditions compared to those associated with SN. Therefore, the preliminary experiments were performed on healthy participants, using a version of the test that simulates apparent symptoms of SN. During SN simulation, all the targets on the left visual field (left side of the computer screen) were hidden to shift the attention to the right side. Therefore, such simulation can be used to study differences in attention to left and right sides of the screen in healthy participants. The nonparametric Wilcoxon test was used to statistically evaluate the differences between the EEG responses due to distractors located on the right and the left side of the screen corresponding to attention and inattention cases respectively. To assess the system's ability to recognize absence or existence of a target based on the EEG data, a two-class problem that utilizes naïve Bayes classifier was formulated. Results showed that the system achieved accuracy exceeding 70%.

## 2. Related work

A unique feature of computerized tests is that they can measure reaction time which provides a quantitative measure that can be used to reflect improvement in attention during the recovery process (Deouell et al., 2005). An example of such tests is a computer-based

system in which participants were asked to press a keyboard button when they observe a white square that could appear in random locations on a black background along the horizontal meridian (Anderson et al., 2000). To imitate the real-life environment, another computer-based test that measures reaction time besides accuracy of detection of a visual target was introduced (Deouell et al., 2005). The presented design, named as Starry Night Test, showed a sequence of targets on a black background comprising continuously changing distractors. In another study, a computerized visual reaction time task was proposed in which a modified version of a driving simulator test was used, which was originally designed to assess attention and executive functions (van Kessel et al., 2010). In this study, participants were instructed to press a button when they observed a rectangle that could appear either on the middle, left or right of the lane. The source of distraction in that task originates from the fact that the participant had to track the lane while doing the task. Vossel and Fink (2016) measured reaction times using a test that contains one target and one distractor represented as white square and white circle respectively. Targets could either be shown on the left or the right side of the screen without a distractor, or with a distractor (white circle) presented simultaneously on the opposite sides of the screen.

Recently, virtual reality (VR) has been employed to design SN assessment tests (Pedroli et al., 2015). A VR version of some classical paper and pencil tests was proposed where the patients had to use a robotic pen to complete the tasks (Fordell et al., 2011). In a different study, a test named as the locomotor obstacle avoidance VR task was designed (Aravind and Lamontagne, 2014). In this task, patients were asked to walk towards a target while avoiding being hit by moving distractors. In the obstacle detection task (Aravind et al., 2015), the patient had to press a joystick button when one of three targets on left, middle or right side approached. Considering that all the computer based methods were developed to be used in clinics, a mobile application, developed to be used in a patient's home, was proposed to assess SN by implementing the traditional cancellation tests in a VR environment (Pallavicini et al., 2015). While these automated tests introduced improvements over pen and paper tests, they still provide limited information about SN severity.

Alternatively, some studies employed fMRI to assess the functionality of the brain with the aim of studying attention (Corbetta et al., 2005). fMRI data was recorded while participants were subjected to a task in which a fixation cross surrounded by a diamond appeared in the center of the screen while a target letter was shown either on the left or the right side of the screen (Kincade et al., 2005). On the other hand, a box car fMRI design was used (Thimm et al., 2006) in which each participant was asked to focus on a central square on a black screen while distractors and targets were appearing on both right and left side of the screen. Another study employed single and dual tasks (Blini et al., 2016b) to discover whether multitasking can show contralesional spatial disorders in stroke patients with damage in the left hemisphere. In the single task, a target could appear on either the left or the right side of a fixation cross while in the dual one target appeared on both sides. Recently, auditory fMRI-based neurofeedback system was designed to assess whether individuals with SN can up-regulate their right visual cortex activity which is originally suppressed due to right parietal stroke (Robineau et al., 2017). The feedback signal was a number from 0 to 10 that the patients attempt to increase by increasing the right visual cortex activity.

However, fMRI does not provide a direct measure for neural activation. Instead, it measures the oxygen consumption in the brain tissues which is coupled with neural activation. That oxygen consumption changes in case of chronic and acute stroke cases (Fridriksson et al., 2006). Moreover, compared to fMRI, EEG is a portable and cost-efficient alternative than can be used for studying visual attention and SN. For healthy participants, EEG was used to study  $\alpha$ -band (8–15 Hz) synchronization over cortical areas related to the attended visual space during visual spatial attention tasks (Rihs et al., 2007). Moreover,  $\alpha$ -band was also employed to study differences in shifts of covert visual attention between the two hemispheres (Treder et al., 2011). Such differences were shown using statistical comparisons between right and left hemispheres electrodes as well as classification problems aimed at identifying direction of attention shift. Another study investigated the feasibility of EEG-based brain computer interface (BCI) that records brain activity in response to covert visuospatial attention (CVSA) orienting paradigm (Tonin et al., 2013). In that BCI, a target is shown either on bottom left or bottom right corner of the screen with a visual feedback that shows the location of the target identified using the EEG signals corresponding to that target. As for the SN studies, transient visual-evoked potentials (VEPs) were recorded from individuals with SN while they observed circular Gabor gratings as stimuli in one of the four visual quadrants of a computer screen (Di Russo et al., 2008). Although statistical analyses were presented to show the differences in the recorded EEG due to visual attention and inattention, these results were not used to develop SN assessment test. In addition, the design assumed that there were no distractors in the environment so it did not simulate a dynamic scenario. In another study, EEG signals were used to find the relationship between spatial and temporal attention (Faugeras and Naccache, 2016). Participants were subjected to 4 different auditory tasks in which they start with binaural auditory cue that might have low or high frequency followed by a monaural target stimulus that can also have low or high frequency. On the other hand, researchers recently investigated EEG-based neurofeedback systems as a tool for rehabilitation of SN. Specifically, patients were asked to reduce their a rhythm amplitude based on a visual feedback represented by a bar graph which height was proportional to the EEG magnitude recorded from electrode at location P4 (Ros et al., 2017). In another study, an EEG-based CVSA BCI (Tonin et al., 2013) was tested using SN patients (Tonin et al., 2017). The objective of this system was to evaluate the BCI performance when controlled by SN patients as well as monitoring the EEG changes for the SN patients across time. Another study used EEG-based neurofeedback system and correlated the changes in a rhythm with the functional connectivity of fMRI salience network (Ros et al., 2013). However, all these SN-related studies were not used to develop SN assessment test that can tell if a stroke patient suffers from SN since all the work done focused on either rehabilitation of SN or studying the EEG as well as reaction time changes across time between the two hemispheres. In light of the above discussions, utilizing the dynamic structure of the Starry Night Test (Deouell et al., 2005) and based on EEG's capability of capturing differences in visual attention, we developed a passive EEG-based SN assessment test and presented a feasibility study with healthy individuals.

### 3. Materials and methods

This section describes proposed SN test design, SN simulation test for healthy participants, EEG system configuration, analysis methods in addition to the dataset description and the experimental procedures.

#### 3.1 SN test design

We designed a variant of the Starry Night Test (Deouell et al., 2005) that provides a quantitative SN evaluation method with the ability of examining both presence and severity of SN. Compared to the original Starry Night Test that depends on keyboard inputs from the user, the proposed test uses the participant's EEG recorded during the visual presentation to assess SN. As seen in Fig. 1, a red dot occupying  $0.22^\circ$  of the participant's visual field was considered as the target. To minimize the risk of seizure that is induced by a specific range of constant frequencies (Fisher et al., 2005), the target was shown on the screen randomly every 700 ms–2200 ms without a specific temporal or frequency pattern.

The screen was divided into a virtual  $8 \times 8$  grid on which targets were displayed as a temporal sequence at 64 possible random locations. A total of 192 targets appeared on the screen corresponding to 3 screen coverages where one screen coverage corresponds to showing a target once on each of the 64 potential locations. As shown in Fig. 1, distractors, represented as smaller green dots occupying  $0.11^\circ$  of the viewing area, appeared randomly for 50–250 ms in random number of cells of the  $8 \times 8$  virtual grid except for the target cell.

Initially at the beginning of each trial, as seen in Fig. 1, a random number of distractors were shown on the screen. At every random period of 50–250 ms, the visibility of a randomly selected distractor out of the potential 64 distractors was toggled. During a trial, a target appeared once on the screen after a randomly chosen delay range of 700 ms–2200 ms in which distractors were continuously changing as described above without any overlap with the target. The target was shown on the screen for 66 ms and a new trial started after the target disappeared.

The visual stimuli presentation was implemented using Psychtoolbox (Brainard, 1997; Pelli, 1997; Kleiner et al., 2007) in MATLAB. A Lenovo ThinkPad W541 laptop with a screen of size 15.6" (13.6"x7.6") and resolution of  $1920 \times 1080$  pixels was used for the SN test. The viewing area employed in the original Starry Night Test was  $16^\circ \times 12^\circ$  of the participant's field of view when the participant viewed the screen from 100 cm away. However, the aspect ratio of our screen was different from the ratio used in the original Starry Night Test. Therefore, our screen could not support exact  $16^\circ \times 12^\circ$  field of view. We formulated an optimization problem that aim to find a viewing distance that will lead to a visual field of view which is closest to  $16^\circ \times 12^\circ$ . This optimization problem is introduced in (1).

$$\begin{aligned} \min & \left( \frac{w}{2x} - \tan 8 \right)^2 + \left( \frac{h}{2x} - \tan 6 \right)^2 \\ \text{s.t. } & x > 0 \end{aligned} \quad (1)$$

where  $w$ ,  $h$  and  $x$  are the screen width, the screen height and the distance from the screen respectively.

This cost function described in (1) seeks to find the viewing distance that minimizes the squared difference between the horizontal field of view of the original test ( $16^\circ$ ) and that of our test as well as the squared difference between the vertical field of view of the original test ( $12^\circ$ ) and that of our test. Solving the optimization problem using the pattern search method (Luenberger and Ye, 2008) yielded a distance  $x$  of 114 cm corresponding to a viewing area of  $17.23^\circ \times 9.74^\circ$ . That is approximately in line with the acute visual angle for the human eye (Mills and Massey, 1999).

### 3.2. SN simulation procedures

We proposed two procedures for SN simulation. The objective behind designing these simulations is to validate the performance of the system on healthy participants and to study differences in attention levels in terms of brain activity over different brain regions for healthy participants. To achieve such aim, the test described in Section 3.1 was modified to simulate left-sided SN.

For both procedures, before starting the experiments, participants were informed that all the targets would appear on the right side of the screen to shift their attention away from the left side of the screen. During the test, all the potential targets on the left side were hidden in order to keep the attention focused on the right side. Moreover, 1/4th of the potential targets on the right-hand side of the screen were also hidden in a random fashion. The right-hand side targets were hidden, because we expect differences in the EEG corresponding to the right and left-hand side hidden targets due to only the attention shift to the right-hand side of the screen, not due to the presence of targets on the right-hand side.

Procedures differ in the fixation point that the participant should focus on during the experiment. In the first procedure, participants were asked to fix their gaze on the center of the screen. Since SN patients orient their body towards the ipsilesional side by approximately  $5^\circ$  (Ferber and Karnath, 1999), we took this into consideration when simulating SN in the second procedure by defining the fixation point as the center of the right part of the screen. That led to shifting the gaze of each participant by around  $4^\circ$ , representing  $1/4$  of the visual field that the screen covers. The two proposed procedures were conducted to examine the effect of shifting gaze to the right side of the screen on attention and information processing.

In addition to studying attention differences with these two procedures, our other aim is to design an EEG-based classifier to differentiate EEG responses due to shown and hidden targets. Therefore, these two simulation procedures yielded preliminary results to predict the feasibility of the test described in Section 3.1 to identify SN.

### 3.3. Data acquisition

One major concern when designing the proposed SN assessment test was minimizing the test time as much as possible considering the fact that the test is intended to be used with stroke patients who might be in hospitals in an early recovery phase. One way to reduce the

test time is to reduce the system setup complexity by reducing the number of electrodes placed on the scalp. Therefore, we chose 17 main electrodes placed according to the 10-10 system over frontal, central, parietal and occipital lobes at positions  $p1$ ,  $Fp2$ ,  $F3$ ,  $F4$ ,  $Fz$ ,  $Fc1$ ,  $Fc2$ ,  $Cz$ ,  $P1$ ,  $P2$ ,  $C1$ ,  $C2$ ,  $Cp3$ ,  $Cp4$ ,  $P5$ ,  $P6$  and  $Oz$ . Left mastoid was used as a reference for the measured EEG signals. The g. USBamp, which is a biosignal amplifier was used in this study. It included 16 24-bit simultaneously sampled channels with an internal digital signal filtering and processing unit and sampling rate up to 38.4 kHz. As the data was collected using 17 electrodes, a slave amplifier was used to record the signal of the  $Oz$  electrode. The data were digitized with a sampling rate of 256 samples/sec and filtered by the amplifier's 8th order bandpass filter with corner frequencies 2, 62 Hz in addition to 4th order notch filters with corner frequencies 58, 62 Hz. Processed data were transferred from the amplifiers to the laptop via USB 2.0.

### 3.4. Pre-processing and feature extraction

The data was further preprocessed using FIR bandpass filter with corner frequencies: 8, 60 Hz. The FIR design was used due to its numerical stability compared to IIR design. The filter was implemented using Kaiser window as it can provide the shortest filter length with the fastest transition compared to other windows such as Hamming and Blackman (Ferdous, 2013).

We employed time and frequency domain analysis for the EEG data acquired from the SN simulation test for 10 healthy participants. Time domain analysis focused mainly on showing differences in attention due to left and right side hidden targets as well as obtaining the system performance measures for classification of EEG corresponding to hidden and shown targets (i.e., time domain features are used to build EEG-based SN detector) while the frequency domain analysis aimed only at showing the statistical differences in attention between left and right side hidden targets. Specifically, pre-processed data segments of 128 samples/segment corresponding to 500 ms measured EEG time-locked to stimulus onset were used for both time and frequency analyses. In frequency domain, average power spectrum values in  $\alpha$ ,  $\beta$  and  $\gamma$  bands of EEG for right and left side hidden targets were calculated using Welch's power spectral density estimate (Welch, 1967). Wilcoxon test with  $p$  value of 0.05 was used to statistically assess average power spectrum values in  $\alpha$ ,  $\beta$  and  $\gamma$  bands due to the left and right side hidden targets. Considering the time domain analysis, EEG pre-processed data of the left and right side hidden targets were statistically compared using Wilcoxon test with  $p$  value of 0.05. In addition, energy of EEG segments corresponding to the left and right side hidden targets was evaluated according to Eq. (2). Finally, a classification problem was formulated to assess the ability of the system to differentiate hidden and shown targets using pre-processed EEG data as features, Wilcoxon test for feature selection and Naïve Bayes for classification. Data was partitioned into training and testing sets using 10-fold cross validation strategy.

$$E = \sum_{i=1}^N |x[n]|^2 \quad (2)$$



Where  $x[n]$  is a finite length EEG signal and  $N$  represents number of samples in  $x[n]$ .

### 3.5. Experimental design and procedures

All research procedures were approved by local Institutional Review Board (IRB) and all participants provided informed consents. Data were collected under the University of Pittsburgh IRB number of PRO15020115. We piloted the system with 10 healthy participants including 6 males and 4 females with ages ranging from 23 to 31 years old with mean of 25.2 years and standard deviation of  $\pm 2.53$  years. An eligible healthy participant was defined as any person who never experienced stroke and had no history of seizure in the last 6 months prior to carrying out the experiment. Participants were seated in a chair at a distance of 114 cm from the screen in a room with the lights on.

During the experiment, each simulation procedure was performed four times. Each time lasted for 5 min with a 2-min break after each time to reduce the effects of fatigue. For 5 randomly selected participants, we started the session by running center fixation procedure twice followed by running right center fixation procedure twice and then repeated this sequence until each procedure was performed 4 times. This scheme was repeated in the same manner for the other 5 participants but with the right center procedure administered twice at the start of the session.

## 4. Results and discussion

Recall that each healthy participant completed tasks under two different procedures: (1) center ( $C$ ) procedure and (2) right center ( $RC$ ) procedure. In this section, we showed analysis results of these simulation procedures. We also showed comparison of both procedures to determine the effect of changing the fixation point on attention level and visual target processing. For each procedure, we presented results of comparing EEG responses due to hidden target stimuli located on the left side of the screen to those on the right side using statistical significance testing. This comparison was performed in both time and frequency domains. In addition, energy levels of EEG segments of the left and right side hidden targets were evaluated and compared. For each procedure, we present performance measures for the classification problem formulated for the healthy participants to assess the ability of the system to detect absence or presence of targets.

For each participant, the four repetitions of each procedure were averaged to give one  $C$ -procedure average and one  $RC$ -procedure average. Considering the EEG data for the 10 participants, 10  $C$ -procedure and 10  $RC$ -procedure 17 channel EEG data were obtained.

### 4.1. Frequency domain analysis

The alpha brain waves represented by frequencies ranging from 8 to 15 Hz are dominant when the eyes are closed and in deep relaxation cases while the beta waves, occupying frequency range of 16–31 Hz, are correlated with anticipation, attention and concentration. Gamma waves starting from 32 Hz up to the end of the spectrum, are associated with high level information processing such as processing of visual, auditory and tactile stimuli (Tatum, 2014). In this paper, the aim behind the frequency domain analysis is to study the relation between the different frequency bands and the attention and processing levels. In the

following subsections, we show frequency domain analysis results of hidden targets for both SN simulation procedures. As mentioned in Section 3.2, we expected that the EEG data in response to the hidden targets on the attended side would be different than the unattended side.

The objective of this analysis is to compare attention levels towards right and left sides of the screen when employing *C* and *RC* procedures in case of hidden targets. Specifically, this analysis will show which procedure is a better simulator for SN. For each participant, features including average power spectrum for  $\alpha$ ,  $\beta$  and  $\gamma$  bands besides  $\frac{\alpha}{\beta}$ ,  $\frac{\alpha}{\gamma}$ , and  $\frac{\beta}{\gamma}$  average power spectrum ratios were calculated for each procedure average EEG data. For each procedure, for every participant, we statistically compared the power spectrum features corresponding to the trials with hidden targets from left hand side and the right hand side by performing the following nonparametric Wilcoxon signed-rank tests (Sidney Siegel, 1956): (i)  $\alpha_{HT}^L$  vs  $\alpha_{HT}^R$ ; (ii)  $\beta_{HT}^L$  vs  $\beta_{HT}^R$ ; (iii)  $\gamma_{HT}^L$  vs  $\gamma_{HT}^R$ ; (iv)  $\left(\frac{\alpha}{\beta}\right)_{HT}^L$  vs  $\left(\frac{\alpha}{\beta}\right)_{HT}^R$ ; (v)  $\left(\frac{\alpha}{\gamma}\right)_{HT}^L$  vs  $\left(\frac{\alpha}{\gamma}\right)_{HT}^R$ ; and (vi)  $\left(\frac{\beta}{\gamma}\right)_{HT}^L$  vs  $\left(\frac{\beta}{\gamma}\right)_{HT}^R$ . Here upper index L and R are used to represent the identities calculated from the EEGs corresponding to the left and right side trials with hidden targets, respectively; and subindex HT represents the trials with hidden targets.

To compare the  $p$  values of the 2 procedures across each brain lobe, the following steps were carried out for each procedure. The electrodes were divided into 4 groups representing 4 brain regions; frontal lobe, parietal lobe, motor cortex, and visual cortex. The minimum  $p$  value obtained across the electrodes located on a certain region was chosen to represent that region. The objective of this step was to identify the lowest significance that could be achieved on each brain region. The 10  $p$  values obtained from the 10 participants at certain regions were combined to give a single  $p$  value using Fisher's combined probability test (Leroy Folks, 1984). This implies that for each procedure, every region is represented by a single  $p$  value as shown in Tables 1 and 2.

For the *RC* procedure, it was obvious that  $p$  values of the parietal lobe electrodes were very low compared to those on frontal lobe, motor cortex, and visual cortex reflecting more activity on that region which is essentially responsible for attention and sensory information processing as seen in Table 2. Although the  $p$  values over the parietal lobe for the *C* procedure were low as shown in Table 1, such values were not low compared to the values over the other brain regions. Such findings showed that the right center procedure would guarantee better shift in attention as well as better information processing for the right side of the screen. On the other hand, the  $p$  values for the visual cortex of *C* and *RC* procedures were significantly high compared to the other brain regions as seen in Tables 1 and 2. Therefore, there were no significant statistical differences on the visual cortex area between right and left side EEGs due to hidden targets which confirms the ability of the participant to see both sides of the screen. However, based on the  $p$  values for the other brain regions specially those belonging to electrodes of the parietal lobe, it is obvious that the participants processed the information corresponding to the right side hidden targets more than that corresponding to the left side.

Alternatively, for each electrode, the  $p$  values obtained across the 10 participants were combined to give a single  $p$  value using Fisher's combined probability test. In addition, ratio of  $p$  values of the two procedures was calculated for each electrode to reflect the amount of change in that value. These ratios showed an obvious change on the parietal lobe as shown in Fig. 2. Such results were in line with our assumption that attention to the right side would be higher in case of right center procedure. Furthermore, the  $\gamma$  band (Fig. 2c) showed the highest change compared to  $\alpha$  and  $\beta$  (Fig. 2a, b). Moreover,  $\alpha/\gamma$ , and  $\beta/\gamma$  showed a prominent change on the head plot especially at the electrodes located on the parietal lobe as shown in Fig. 2e, f.  $\gamma$  band, which is associated with information processing, is the common factor between these ratios. It can be concluded that there is a major difference in the information processing level represented by the  $\gamma$  waves between the two procedures.

## 4.2 Time domain analysis

Similar to Section 4.1, our aim was to show the procedure with better SN simulation capability (i.e., we aim to compare the SN simulation capabilities of  $C$  and  $RC$  fixation procedures). We conducted Wilcoxon test to determine if there was a significant difference in pre-processed EEG segments corresponding to right and left side hidden targets. Such statistical comparison was performed for both  $C$  and  $RC$  fixation procedures. Results showed that there was a significant difference at specific time points ( $\approx 150$  ms and 200 ms). These points form a N100/P200 combination indicated by black crosses as seen in Fig. 3 where N100 is a negative wave that occurs after 100 ms from the onset of the stimulus while the P200 is a positive wave that occurs after 200 ms from the onset of the stimulus. Such combination of N100 and P200 reflects attention state (Sur and Sinha, 2009). In the  $RC$  procedure, there was a larger number of significant points forming N100/P200 combination compared to the number of significant points obtained in  $C$  procedure as seen in Fig. 3a and b. The amplitude difference between the preprocessed EEG signals of the right and the left side hidden targets was greater for the  $RC$  procedure compared to the  $C$  procedure giving a stronger N100/P200 attention response.

To reveal more differences between the two procedures, differences in average energy of the 10 participants between  $RC$  and  $C$  procedures were calculated across each brain region. Average energy of the right side hidden targets across the 10 participants for the  $C$  procedure was subtracted from average energy of the right side hidden targets for the  $RC$  procedure. The same energy difference was calculated for left side hidden targets. Considering Table 3, average energy difference between  $RC$  and  $C$  procedures of the right side hidden targets is higher than that of the left side hidden targets. Moreover, it was noted that the highest energy difference between  $RC$  and  $C$  procedures occurred in the parietal lobe reflecting the fact that the main difference between the two procedures is mainly related to attention and sensory information processing. The negative sign of the left side energy difference confirmed that the left side showed less energy in case of  $RC$  fixation. In other words, the left side hidden targets received less attention in case of  $RC$  procedure and thus produced less activation compared to those in the  $C$  fixation procedure. Both temporal and spectral analyses show that  $RC$  procedure is a better SN simulator.

Next, for both simulation procedures, to assess the ability of the system to recognize shown and hidden targets based on the EEG data, a simple two-class problem that utilizes Wilcoxon test and naïve Bayes classifier was formulated. Distinguishing between hidden and shown targets allow us to detect if there is SN. Here, detecting if the targets are hidden simulates the case in which the participant neglected the targets while detecting if the targets are shown represents the case in which the participant perceived the targets. For this reason, we define sensitivity as the accuracy of detecting the perceived targets. Similarly, specificity is defined as the accuracy identifying the neglected targets. Overall accuracy shows the identification among perceived and neglected signals. Performance measures showed that the sensitivity was higher for *RC* sessions (Table 4) whereas accuracy and specificity were higher for *RC* sessions in 7/10 participants. *RC* experiments achieved average accuracy, sensitivity and specificity of 74.24%, 75.17% and 71.36% respectively while the *C* procedure obtained average accuracy, sensitivity and specificity of 70.91%, 71.56% and 68.87 respectively. The sensitivity difference between the two procedures is in agreement with the claim explained before that the *RC* procedure showed higher level of attention and target processing compared to the *C* procedure.

This study had several limitations. In particular, the attention shift performed by the healthy participants during SN simulation is voluntary while SN is not a voluntary phenomenon since the patient is not aware of his/her shift of attention. Moreover, our approach to simulating SN may have provided a less realistic simulation compared to other methods, such as the use of prism glasses (Schintu et al., 2014). However, our approach was the most compatible with our Starry Night EEG SN assessment test. More specifically, the proposed SN assessment test was modified to be tested initially with healthy participants through SN simulation to predict the feasibility of the proposed SN assessment test when used with patients. If we used prism adaptation for SN simulation, the obtained performance measures using healthy participants cannot be used as a prediction of the performance measures obtained by the proposed SN assessment test when tested with patients since, in this case, the SN simulation test (prism adaptation) will be different than the SN assessment test (Starry Night). Moreover, we did not account for pseudo-neglect (Nicholls et al., 2017); a phenomenon in which some healthy individuals over attend to the left side. In contrast, in this study, we try to shift the participant's attention away from the left side of the screen using both center and right center procedures. For instance, if a participant experiences pseudo-neglect, this will not improve the analysis results. Instead, it will yield less significance when statistically comparing left and right side visual fields. Consequently, worse performance measures would be obtained. However, we obtained average accuracy of 74.24% when analyzing the healthy individuals' data as seen in Table 4. We think that the results obtained from this study are promising and justify exploration of this approach with a sample of individuals with stroke.

## 5. Conclusion

In this paper, we presented a feasibility study for a novel EEG-based SN assessment test using identification of missed stimuli within the available field of vision. The potential benefits of this test, particularly its ability to provide more information on SN severity, bear further exploration in a sample of individuals with SN following stroke. The preliminary

results for healthy participants showed that when the SN was simulated, the proposed system achieved successful separation between the hidden (neglected) and shown (observed) stimuli especially when participants were asked to focus on the center of the right part of the screen during data collection. In such case, the system achieved average accuracy, sensitivity and specificity of 74.24%, 75.17% and 71.36% respectively. In addition, results showed that there are significant differences in attention when comparing EEG responses corresponding to right and left side hidden targets especially on the parietal lobe which is responsible for attention and high-level information processing. Moreover, N100/P200 combination reflecting the attention component was found in the EEG segments corresponding to hidden targets on the right side of the screen.

To go beyond a feasibility study and to further test the system, the next step in our work will focus on validating the EEG SN assessment system with patients experiencing SN. In this paper, our sample included young participants (mean age of 25 years) with no brain pathology. We need to ensure that the results achieved in healthy participants will generalize to the older and more impaired population seen in clinical stroke rehabilitation settings. Moreover, there are certain issues from both clinical and engineering perspective that we will further investigate. For example, we will assess the system performance when the size, type and location of the brain lesion varies. Future work will also include sophisticated analysis methods such as vector autoregressive models (VARs) (Lütkepohl, 2005) to show the relationships among signals originating from different brain regions and provide a functional connectivity map that will reveal how the electrical activity originates and transfers through brain lobes for those who suffer from SN. Furthermore, EEG microstate analysis will be performed to compare neural activity across subjects based on spatiotemporal patterns of EEG microstates (Zappasodi et al., 2017). Finally, the proposed test will be used to develop an EEG-based gaze controlled virtual reality SN assessment environment with neurofeedback training within the context of dynamic, functional activities to speed up the recovery process of patients with SN.

## References

- Agis D, Goggins MB, Oishi K, Oishi K, Davis C, Wright A, Kim EH, Sebastian R, Tippett DC, Faria A, Hillis AE, 2016 Picturing the size and site of stroke with an expanded national institutes of health stroke scale. *Stroke* 47, 1459–1465, 10.1161/STROKEAHA.115.012324. [PubMed: 27217502]
- Anderson B, Menneer M, Chatterjee A, 2000 Variability not ability: another basis for performance decrements in neglect. *Neuropsychologia* 38, 785–796, 10.1016/S0028-3932(99)00137-2. [PubMed: 10689054]
- Aravind G, Lamontagne A, 2014 Perceptual and locomotor factors affect obstacle avoidance in persons with visuospatial neglect. *J. Neuroeng. Rehabil* 11, 38, 10.1186/1743-0003-11-38. [PubMed: 24645796]
- Aravind G, Darekar A, Fung J, Lamontagne A, 2015 Virtual reality-based navigation task to reveal obstacle avoidance performance in individuals with visuospatial neglect. *EEE Trans. Neural Syst. Rehabil. Eng* 23, 179–188, 10.1109/TNSRE.2014.2369812.
- Baldassarre, et al., 2014 Large-scale changes in network interactions as a physiological signature of spatial neglect. *Brain* 137, 3267–3283, 10.1093/brain/awu297. [PubMed: 25367028]
- Becker E, Karnath H-O, 2007 Incidence of visual extinction after left versus right hemisphere stroke. *Stroke* 38, 3172–3174, 10.1161/STROKEAHA.107.489096. [PubMed: 17962601]

- Blini E, Romeo Z, Spironelli C, Pitteri M, Meneghello F, Bonato M, Zorzi M, 2016a Multi-tasking uncovers right spatial neglect and extinction in chronic left-hemisphere stroke patients. *Neuropsychologia* 92, 147–157, 10.1016/j.neuropsychologia.2016.02.028. [PubMed: 26948071]
- Blini E, Romeo Z, Spironelli C, Pitteri M, Meneghello F, Bonato M, Zorzi M, 2016b Multi-tasking uncovers right spatial neglect and extinction in chronic left-hemisphere stroke patients. *Neuropsychologia*, 10.1016/j.neuropsychologia.2016.02.028.
- Bonato M, Deouell LY, 2013 Hemispatial neglect: computer-based testing allows more sensitive quantification of attentional disorders and recovery and might lead to better evaluation of rehabilitation. *Front. Hum. Neurosci* 7, 162, 10.3389/fnhum.2013.00162. [PubMed: 23641207]
- Brainard DH, 1997 The Psychophysics Toolbox. *Spatial Vision* 10, 433–436. [PubMed: 9176952]
- Brouwer A-M, van Erp J, Heylen D, Jensen O, Poel M, 2013 Effortless Passive BCIs for Healthy Users. Springer, Berlin Heidelberg, pp. 615–622, 10.1007/978-3-642-39188-0\_66.
- CDC, NCHS, 2015 Underlying Cause of Death 1999–2014 on CDC WONDER Online Database [WWW Document]. URL <http://wonder.cdc.gov/ucd-icd10.html> (Accessed 19 December 2017).
- Committeri G, Pitzalis S, Galati G, Patria F, Pelle G, Sabatini U, Castriota-Scanderbeg A, Piccardi L, Guariglia C, Pizzamiglio L, 2007 Neural bases of personal and extrapersonal neglect in humans. *Brain* 130, 431–441. [PubMed: 17008330]
- Corbetta M, Kincade MJ, Lewis C, Snyder AZ, Sapir A, 2005 Neural basis and recovery of spatial attention deficits in spatial neglect. *Nat. Neurosci* 8, 1603–1610, 10.1038/nn1574. [PubMed: 16234807]
- Deouell LY, Sacher Y, Soroker N, 2005 Assessment of spatial attention after brain damage with a dynamic reaction time test. *J. Int. Neuropsychol. Soc* 11, 697–707, 10.1017/S1355617705050824. [PubMed: 16248905]
- Di Russo, et al., 2008 Impaired visual processing of contralesional stimuli in neglect patients: a visual-evoked potential study. *Brain* 131, 842–854, 10.1093/brain/awm281. [PubMed: 18024488]
- Donnan Geoffrey A., et al., 2008 Stroke. *Lancet* 371, 1612–1623, 10.1016/S0140-6736(08)60694-7. [PubMed: 18468545]
- Faugeras F, Naccache L, 2016 Dissociating temporal attention from spatial attention and motor response preparation: a high-density EEG study. *Neuroimage* 124, 947–957, 10.1016/j.neuroimage.2015.09.051. [PubMed: 26433120]
- Ferber S, Karnath HO, 1999 Parietal and occipital lobe contributions to perception of straight a head orientation. *J. Neurol. Neurosurg. Psychiatry* 67, 572–578. [PubMed: 10519859]
- Ferdous J, 2013 A Survey Report for Performance Analysis of Finite Impulse Response Digital Filter by Using Different Window Techniques, pp. 265–270.
- Fisher RS, Harding G, Erba G, Barkley GL, Wilkins A, 2005 Photic- and pattern-induced seizures: a review for the epilepsy foundation of america working group. *Epilepsia* 46, 1426–1441, 10.1111/j.1528-1167.2005.31405.x. [PubMed: 16146439]
- Fordell H, Bodin K, Bucht G, Malm J, 2011A virtual reality test battery for assessment and screening of spatial neglect. *Acta Neurol. Scand* 123, 167–174, 10.1111/j.1600-0404.2010.01390.x. [PubMed: 20569225]
- Fridriksson J, Rorden C, Morgan P, Leigh Morrow K, Baylis G, 2006 Measuring the hemodynamic response in chronic hypoperfusion. *Neurocase* 12, 146–150, 10.1080/13554790600598816. [PubMed: 16801150]
- Grimes D, Tan DS, Hudson SE, Shenoy P, Rao RPN, 2008 Feasibility and pragmatics of classifying working memory load with an electroencephalograph. In: *Proceeding of the Twenty-Sixth Annual CHI Conference on Human Factors in Computing Systems – CHI '08*, ACM Press, New York, New York, USA, 10.1145/1357054.1357187, p. 835.
- Heilman KM, Watson RT, Valenstein E, 1993 Neglect and related disorders. *Clin. Neuropsychol* 3, 279–336.
- Kincade JM, Abrams RA, Astafiev SV, Shulman GL, Corbetta M, 2005 An event-related functional magnetic resonance imaging study of voluntary and stimulus-driven orienting of attention. *J. Neurosci* 25, 4593–4604, 10.1523/JNEUROSCI.0236-05.2005. [PubMed: 15872107]
- Kleiner M, Brainard D, Pelli D, 2007 “What’s new in Psychtoolbox-3?” *Perception* 36 ECVF Abstract Supplement.

- Lütkepohl H, 2005 New Introduction to Multiple Time Series Analysis, New Introduction to Multiple Time Series Analysis. Springer Berlin Heidelberg, Berlin, Heidelberg.
- Leroy Folks J, 1984 6 Combination of independent tests. *Handb. Stat* 4, 113–121, 10.1016/S0169-7161(84)04008-6.
- Li K, Malhotra PA, 2015 Spatial neglect. *Pract. Neurol* 15, 333–339, 10.1136/practneurol-2015-001115. [PubMed: 26023203]
- Luenberger DG, Ye Y, 2008 Linear and Nonlinear Programming, International Series in Operations Research {&} Management Science. Springer, US, Boston, MA, 10.1007/978-0-387-74503-9\_15.
- Mills SL, Massey SC, 1999 All amacrine cells limit scotopic acuity in central macaque retina: a confocal analysis of calretinin labeling. *J. Comp. Neurol* 411, 19–34. [PubMed: 10404105]
- Nicholls MER, Hobson A, Petty J, Churches O, Thomas NA, 2017 The effect of cerebral asymmetries and eye scanning on pseudoneglect for a visual search task. *Brain Cogn.* 111, 134–143, 10.1016/j.bandc.2016.11.006. [PubMed: 27923149]
- Pallavicini F, Pedroli E, Serino S, Dell’Isola A, Cipresso P, Cisari C, Riva G, 2015 Assessing Unilateral Spatial Neglect using advanced technologies: the potentiality of mobile virtual reality. *Technol. Health Care* 23, 795–807, 10.3233/THC-151039. [PubMed: 26409526]
- Pedroli E, Serino S, Cipresso P, Pallavicini F, Riva G, 2015 Assessment and rehabilitation of neglect using virtual reality: a systematic review. *Front. Behav. Neurosci* 9, 226, 10.3389/fnbeh.2015.00226. [PubMed: 26379519]
- Pelli DG, 1997 The VideoToolbox software for visual psychophysics: transforming numbers into movies. *Spatial Vision* 10, 437–442. [PubMed: 9176953]
- Plummer P, Morris ME, Dunai J, 2003 Assessment of unilateral neglect. *Phys. Ther* 83, 732–740, 10.1037/0894-4105.4.2.87. [PubMed: 12882614]
- Rihs TA, Michel CM, Thut G, 2007 Mechanisms of selective inhibition in visual spatial attention are indexed by alpha-band EEG synchronization. *Eur. J. Neurosci* 25, 603–610, 10.1111/j.1460-9568.2007.05278.x. [PubMed: 17284203]
- Robineau F, Saj A, Neveu R, Van De Ville D, Scharnowski F, Vuilleumier P, 2017 Using real-time fMRI neurofeedback to restore right occipital cortex activity in patients with left visuo-spatial neglect: proof-of-principle and preliminary results. *Neuropsychol. Rehabil.* 1–22, 10.1080/09602011.2017.1301262.
- Ros T, Théberge J, Frewen PA, Kluetsch R, Densmore M, Calhoun VD, Lanius RA, 2013 Mind over chatter: plastic up-regulation of the fMRI salience network directly after EEG neurofeedback. *Neuroimage* 65, 324–335, 10.1016/j.neuroimage.2012.09.046. [PubMed: 23022326]
- Ros T, Michela A, Bellman A, Vuadens P, Saj A, Vuilleumier P, 2017 Increased alpha-rhythm dynamic range promotes recovery from visuospatial neglect: a neurofeedback study. *Neural Plast.* 7407241, 10.1155/2017/7407241. [PubMed: 28529806]
- Schintu S, Pisella L, Jacobs S, Saleme R, Reilly KT, Farne A, 2014 Prism adaptation in the healthy brain: the shift in line bisection judgments is long lasting and fluctuates. *Neuropsychologia* 53, 165–170, 10.1016/j.neuropsychologia.2013.11.013. [PubMed: 24291512]
- Schmidt EA, Schrauf M, Simon M, Fritzsche M, Buchner A, Kincses WE, 2009 Drivers’ misjudgement of vigilance state during prolonged monotonous daytime driving. *Accid. Anal. Prev* 41, 1087–1093, 10.1016/j.aap.2009.06.007. [PubMed: 19664450]
- Seki K, Ishiai S, 1996 Diverse patterns of performance in copying and severity of unilateral spatial neglect. *J. Neurol* 243, 1–8. [PubMed: 8869379]
- Siegel Sidney, 1956 Nonparametric Statistics for the Behavioral Sciences ebook «Mara’s Life. McGraw-Hill, New York.
- Sur S, Sinha VK, 2009 Event-related potential: an overview. *Ind. Psychiatry J.* 18, 70–73, 10.4103/0972-6748.57865.
- Tatum WO, 2014 Ellen R: grass lecture: extraordinary EEG. *Neurodiagn. J* 54, 3–21. [PubMed: 24783746]
- Thimm M, Fink GR, Küst J, Karbe H, Sturm W, 2006 Impact of alertness training on spatial neglect: a behavioural and fMRI study. *Neuropsychologia* 44, 1230–1246, 10.1016/j.neuropsychologia.2005.09.008. [PubMed: 16280140]

- Tonin L, Leeb R, Sobolewski A, Millán J, del R, 2013 An online EEG BCI based on covert visuospatial attention in absence of exogenous stimulation. *J. Neural Eng* 10, 056007, 10.1088/1741-2560/10/5Z056007. [PubMed: 23918205]
- Tonin L, Pitteri M, Leeb R, Zhang H, Menegatti E, Piccione F, Millán JDR, 2017 Behavioral and cortical effects during attention driven brain-computer interface operations in spatial neglect: a feasibility case study. *Front. Hum. Neurosci* 11, 336, 10.3389/fnhum.2017.00336. [PubMed: 28701939]
- Treder MS, Bahramisharif A, Schmidt NM, van Gerven MAJ, Blankertz B, 2011 Brain-computer interfacing using modulations of alpha activity induced by covert shifts of attention. *J. Neuroeng. Rehabil* 8, 24, 10.1186/1743-0003-8-24. [PubMed: 21672270]
- Unsworth CA, 2006 In: O'Sullivan SB, Schmitz TJ (Eds.), *Physical Rehabilitation: Assessment and Treatment*, pp. 1149–1188, Philadelphia.
- van Kessel ME, van Nes IJW, Brouwer WH, Geurts ACH, Fasotti L, 2010 Visuospatial asymmetry and non-spatial attention in subacute stroke patients with and without neglect. *Cortex* 46, 602–612. [PubMed: 19591978]
- Vossel S, Fink GR, 2016 Contralesional distractors enhance ipsilesional target processing after right-hemispheric stroke. *Cortex* 78, 115–124. [PubMed: 27035700]
- Welch P, 1967 The use of fast Fourier transform for the estimation of power spectra: a method based on time averaging over short, modified periodograms. *IEEE Trans. Audio Electroacoust* 15, 70–73, 10.1109/TAU.1967.1161901.
- Wilson B, Cockburn J, Halligan P, 1987 Development of a behavioral test of visuospatial neglect. *Arch. Phys. Med. Rehabil* 68, 98–102. [PubMed: 3813864]
- Zander T, Kothe C, 2011 Towards passive brain-computer interfaces: applying brain-computer interface technology to human-machine systems in general. *J. Neural Eng* 8, 025005, 10.1088/1741-2560/8/2/025005. [PubMed: 21436512]
- Zappasodi F, Croce P, Giordani A, Assenza G, Giannantoni NM, Profice P, Granata G, Rossini PM, Tecchio F, 2017 Prognostic value of EEG microstates in acute stroke. *Brain Topogr.* 30, 698–710, 10.1007/s10548-017-0572-0. [PubMed: 28547185]



**HIGHLIGHTS**

- We propose an objective EEG-based neglect assessment test.
- Our test does not require physical input from patients unlike traditional tests.
- We studied the feasibility of the proposed test with healthy individuals.
- Attention to left and right sides of the screen was evaluated statistically.
- Average accuracy of 74.24% was achieved.

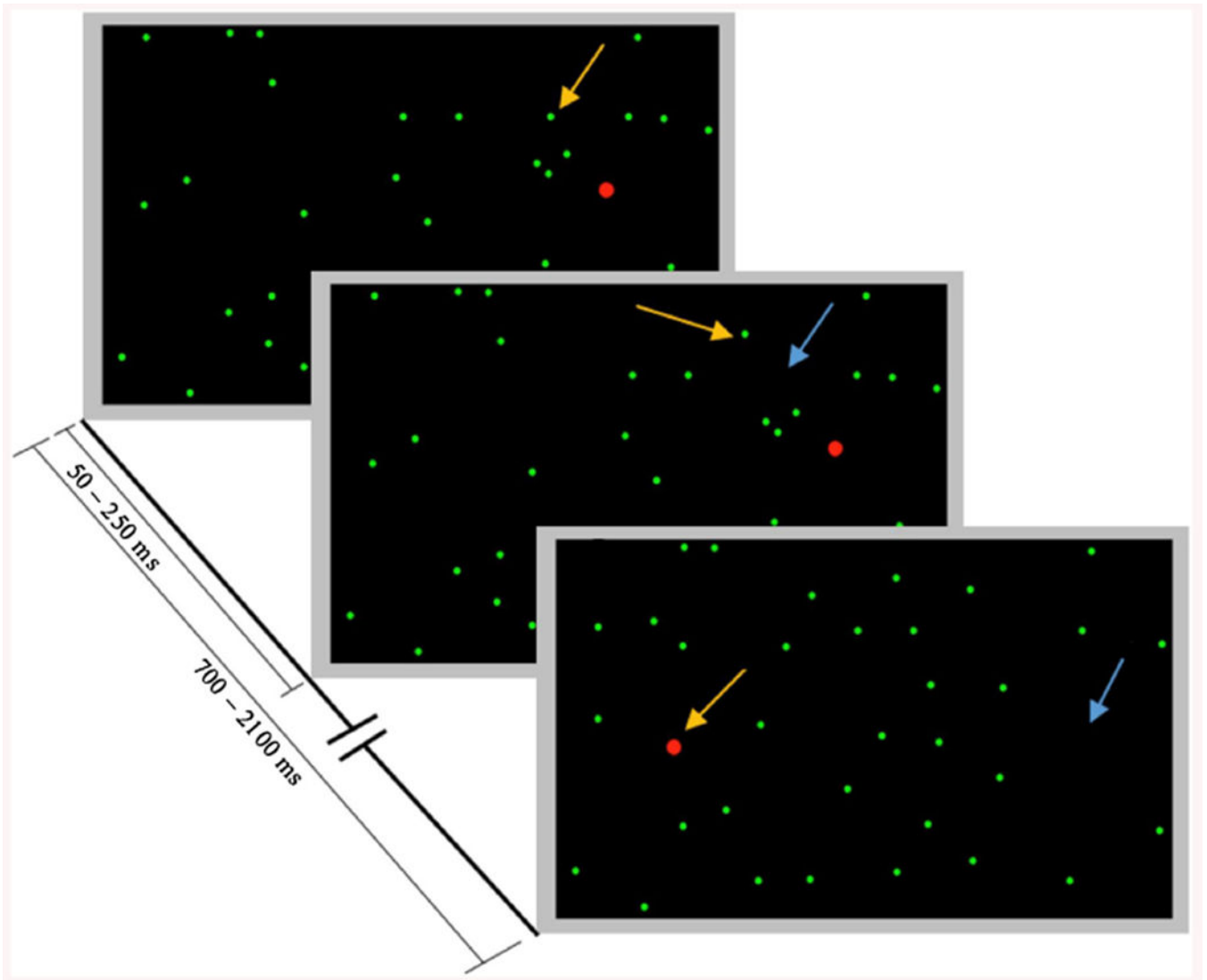


**Fig. 1.**

One trial of the Starry Night Test in which the targets are shown as red dots that are bigger in size than the green dots representing distractors. Arrows indicate locations of change in each frame (a yellow arrow indicates appearance of an object while a blue arrow indicates disappearance of an object). This figure is a modified form of the one showing the original Starry Night Test (Deouell et al., 2005). (For interpretation of the references to colour in this figure legend, the reader is referred to the web version of this article.)

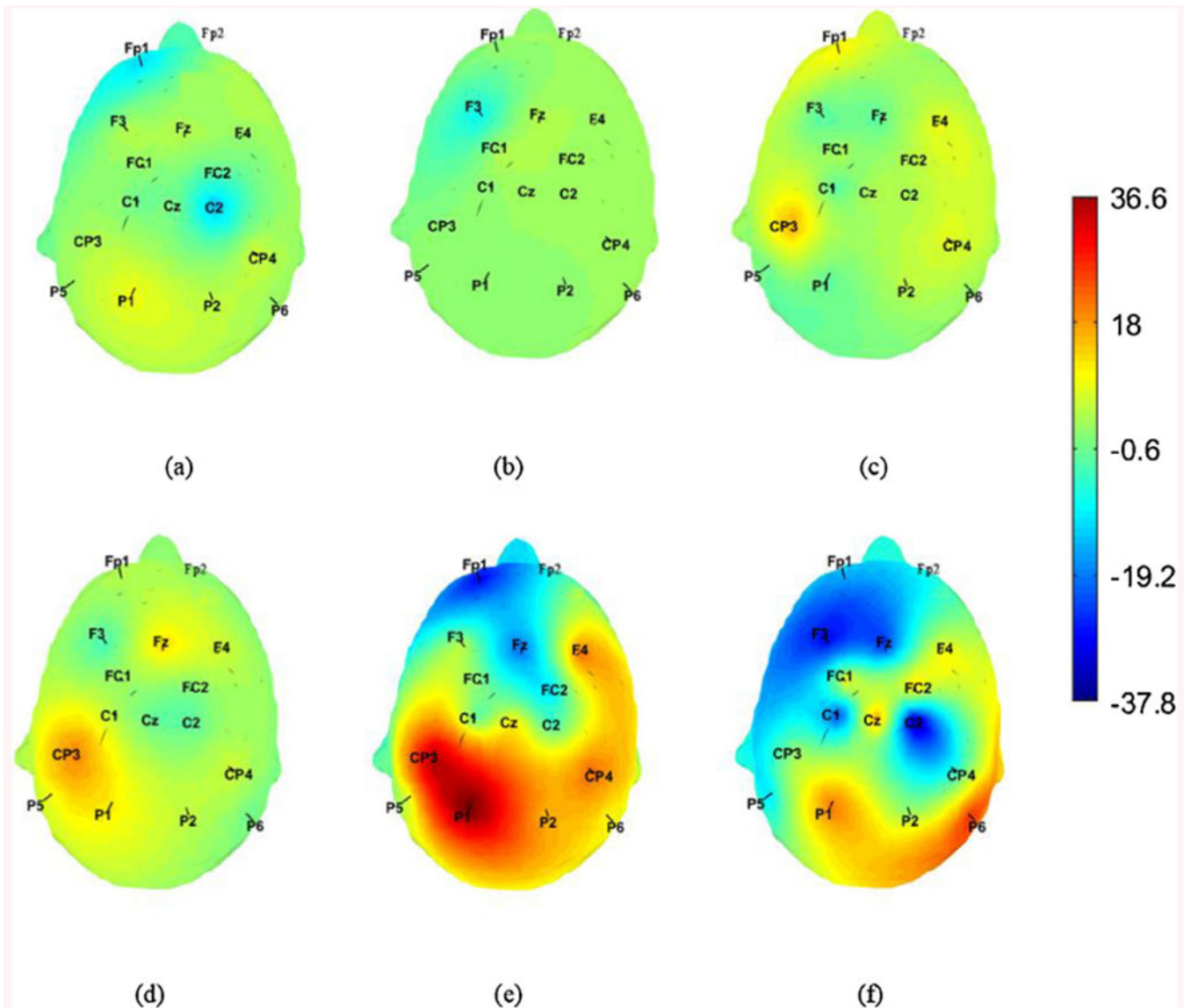
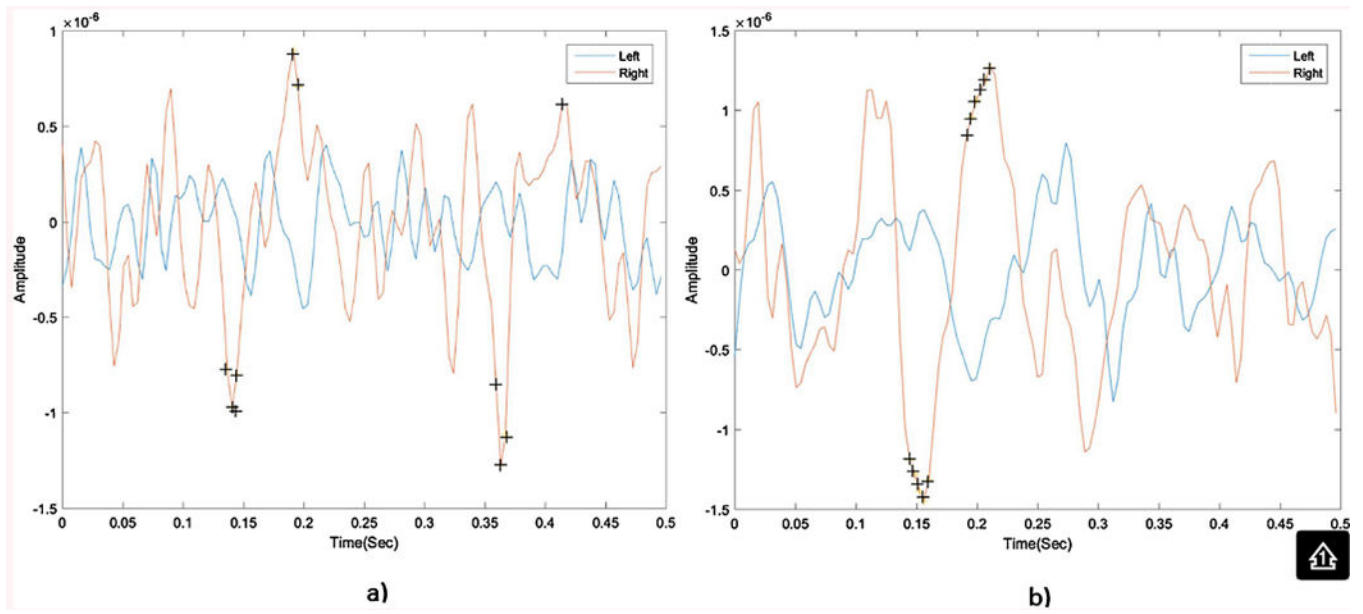


Fig. 2.

Heat map for the p values of the center procedure divided by the P values for the right center one at each electrode location for a)  $\frac{\alpha_c}{\alpha_{RC}}$ , b)  $\frac{\beta_c}{\beta_{RC}}$ , c)  $\frac{\gamma_c}{\gamma_{RC}}$ , d)  $\frac{(\alpha/\beta)_C}{(\alpha/\beta)_{RC}}$ , e)  $\frac{(\alpha/\gamma)_C}{(\alpha/\gamma)_{RC}}$  f)  $\frac{(\beta/\gamma)_C}{(\beta/\gamma)_{RC}}$ .

All ratios were logarithmically scaled before plotting.



**Fig. 3.**  
Average 500 ms EEG signals for right and left side hidden targets collected from *Cp3* electrode with significant points indicated by a plus sign(+) for 1- center procedure (a) 2- right center procedure (b).

**Table 1**

Combined P values of average power spectrum features for center procedure comparing right and left side hidden targets.

<b>P value</b>	<b><math>\alpha</math></b>	<b>B</b>	<b><math>\gamma</math></b>	<b><math>\alpha/\beta</math></b>	<b><math>\alpha/\gamma</math></b>	<b><math>B/\gamma</math></b>
Frontal Lobe	$10^{-21}$	$10^{-9}$	$10^{-11}$	$10^{-21}$	$10^{-51}$	$10^{-52}$
Motor cortex	$10^{-12}$	$10^{-2}$	$10^{-13}$	$10^{-9}$	$10^{-46}$	$10^{-44}$
Parietal Lobe	$10^{-20}$	$10^{-2}$	$10^{-10}$	$10^{-14}$	$10^{-50}$	$10^{-48}$
Visual Cortex	0.08	0.9	$10^{-5}$	0.006	$10^{-12}$	$10^{-15}$

Author Manuscript

Author Manuscript

Author Manuscript

Author Manuscript

**Table 2**

Combined P values of average power spectrum features for right center procedure comparing right and left side hidden targets.

P value	$\alpha$	B	$\gamma$	$\alpha/\beta$	$\alpha/\gamma$	$\beta/\gamma$
Frontal Lobe	$10^{-16}$	$10^{-6}$	$10^{-11}$	$10^{-18}$	$10^{-43}$	$10^{-50}$
Motor cortex	$10^{-11}$	$10^{-4}$	$10^{-6}$	$10^{-13}$	$10^{-42}$	$10^{-42}$
Parietal Lobe	$10^{-19}$	$10^{-7}$	$10^{-13}$	$10^{-20}$	$10^{-55}$	$10^{-53}$
Visual Cortex	0.02	0.697	$10^{-4}$	$10^{-4}$	$10^{-11}$	$10^{-15}$

Author Manuscript

Author Manuscript

Author Manuscript

Author Manuscript

**Table 3**

Average energy difference between right center and center procedures for both right and left side hidden targets.

<b>Brain Region</b>	<b>Right side energy difference x10<sup>-10</sup></b>	<b>Left side energy difference x10<sup>-11</sup></b>
Frontal Lobe	2.61	-7.44
Motor cortex'	2.45	-10.04
Parietal Lobe	2.75	-7.98
Visual Cortex Energy	1.62	9.68

Author Manuscript

Author Manuscript

Author Manuscript

Author Manuscript

**Table 4**

Performance measures of the proposed test for healthy participants for both right center and center procedures.

Participant	Fixation Point	Accuracy	Specificity	Sensitivity
HC01	Center	74.80%	72.26%	75.62%
	Right Center	<b>79.37%</b>	<b>80.00%</b>	<b>79.17%</b>
HC02	Center	68.19%	<b>64.19%</b>	69.48%
	Right Center	<b>69.06%</b>	63.87%	<b>70.73%</b>
HC03	Center	65.35%	59.35%	67.29%
	Right Center	<b>70.39%</b>	<b>66.45%</b>	<b>71.67%</b>
HC04	Center	72.60%	73.55%	72.29%
	Right Center	<b>78.66%</b>	<b>75.16%</b>	<b>79.79%</b>
HC05	Center	72.13%	<b>71.29%</b>	72.40%
	Right Center	<b>75.04%</b>	68.39%	<b>77.19%</b>
HC06	Center	<b>68.19%</b>	<b>65.81%</b>	68.96%
	Right Center	67.95%	62.26%	<b>69.79%</b>
HC07	Center	71.89%	70.00%	72.50%
	Right Center	<b>78.82%</b>	<b>84.84%</b>	<b>76.87%</b>
HC08	Center	74.17%	73.55%	74.34%
	Right Center	<b>81.73%</b>	<b>90.00%</b>	<b>79.06%</b>
HC09	Center	<b>71.42%</b>	<b>71.94%</b>	71.25%
	Right Center	68.98%	51.29%	<b>74.69%</b>
HC10	Center	70.31%	66.77%	71.46%
	Right Center	<b>72.36%</b>	<b>71.29%</b>	<b>72.71%</b>

For each subject HCx, two accuracies, sensitivities, and specificities are calculated. The highest accuracy, sensitivity, and specificity are written in bold.